Journal of
Mechanical
Science and
Technology

Journal of Mechanical Science and Technology 21 (2007) 403~414

Analysis of an Unsteadily Propagating Crack under Mode I and II Loading

Kwang Ho Lee[a,*], Gap Su Ban[a]

[a]*Department of Automotive Engineering , Sangju National University, Kyungbuk, 742-711, Korea*

(Manuscript Received May 24, 2006; Revised January 8, 2007; Accepted January 10, 2007)

Abstract

Stress and displacement fields for an unsteadily propagating crack under mode I and II loading are developed through an asymptotic analysis. Dynamic equilibrium equations for the unsteady state are developed and the solution to the displacement fields and the stress fields for a crack propagating with high crack tip acceleration, deceleration and rapidly varying stress intensity factor. The influence of transients on the higher order terms of the stress fields are explicitly revealed. Using these stress components, isochromatic fringes around the propagating crack are generated for different crack speeds, crack tip accelerations and the time rate of change of stress intensity factor, and the effects of the transients on these fringes are discussed. The effects of the transients on the dynamic stress intensity factor are discussed when a crack propagates with high acceleration and deceleration. The effect of transient on the time rate of change of dynamic stress intensity factor below Rayleigh wave speed in an infinite body is also studied.

Keywords: Unsteady crack propagation, Dynamic stress intensity factor, Stress and displacement fields, Isochromatic fringes, Acceleration and deceleration crack, Time rate of change of dynamic stress intensity factor

1. Introduction

Dynamic fractures analysis can be classified into stationary and propagating crack problems. In case of dynamic stationary crack problem, the stress and displacement fields are time dependent. Thus, the stress intensity factors are vary with time. A dynamic propagating crack problem can be divided into steady and unsteady states. Generally, in the steady state, stresses and displacements depend, not on time, but crack propagation velocity. However, in the unsteady dynamic state, they are variable with time. Thus, dynamic stress intensity factor (DSIF) and crack propagation velocity in the unsteady state changes with time, and the transient phenomena occur mainly at the starting and stopping crack.

The structure of dynamic stress and displacement fields for a stationary crack tip was studied by Thau and Lu (1971), Sih and Embley (1972), Chen (1978), Itou (1980) using a Laplace-Fourier variable method and their results indicate that the dynamic fields are the same as static ones, except for the stress intensity factor which is time dependent.

The structure of dynamic stress and displacement fields for a propagating crack tip was studied by Yoffe (1951), Craggs (1960), Nishioka et al. (1983) and Lee et al. (1996) and their results indicate that the crack tip stress fields retain the inverse square root singularity and is dependent on the instantaneous value of the stress intensity factor and the crack propagation velocity.

However, Dally and Shukla's experiment (1979) shows that the crack tip fields are dependent on the

*Corresponding author. Tel.: +82 54 530 5404; Fax.: +82 54 530 5407
E-mail address: khlee@sangju.ac.kr

high crack tip acceleration and rapidly varying stress intensity factor in addition to instant stress intensity factor and crack propagation velocity. In all these studies, the crack propagates at constant velocity in steady state. Since the crack tip speed changes rapidly during crack initiation, the crack growth is likely to be transient, with the crack speed and dynamic stress intensity factors changing as a function of time. Using the two wave displacement potentials, Freund (1990) provided the partial differential equations and the solutions for two wave potentials in the dynamic equilibrium and a higher order asymptotic expansion for the first stress invariant and Guo et al. (2003) analyzed for sudden jumps in the crack tip velocity by numerical and experiment. Ing and wang (2004) investigated for transient response of a mode III crack propagating in a piezoelectric medium. In spite of these studies, the understanding of the individual stresses and displacements for a propagating transient crack is still limited. Rosakis, Liu and Freund (1991) obtained the higher order asymptotic individual stress components near the tip of a non-uniformly propagating mode I crack. However, their solutions can't have harmonic function because of being obtained from not transformed Laplace's equation but general differential equation in the dynamic equilibrium. When we generate the contours for constant maximum shear stress (isochromatics) for mode I using their individual stress fields under high crack tip acceleration and rapidly varying stress intensity factor, the isochromatics can't be symmetric about the x-axis on the basis of crack tip.

To overcome this problem, the stress and displacement fields for a transiently propagating crack are developed through a new method in this paper. The transient equilibrium equation is formulated in terms of displacement potentials and the solution is obtained through an asymptotic analysis. In analyzing this problem, it is very important that one transforms the general partial differential equation in the dynamic equilibrium into the Laplace's equation whose solution has harmonic function. The method of this transform is first proposed in this paper. From the solutions of the Laplace's equations, the stress and displacement fields for a transient crack are obtained. Using the stress fields developed in this study, the contours for the isochromatics are generated and the effects of a transient crack on these contours are discussed.

2. Stress and displacement fields for an unsteadily propagating crack

2.1. Formation for equilibrium equations

The relationship between stress and strain can be written as

$$\begin{aligned}\sigma_{XX} &= C_{11}\varepsilon_{XX} + C_{12}\varepsilon_{YY}\\ \sigma_{YY} &= C_{12}\varepsilon_{XX} + C_{11}\varepsilon_{YY}\\ \tau_{XY} &= C_{66}\gamma_{XY}\end{aligned} \tag{1}$$

where $\boldsymbol{X}$ and Y are `the reference coordinates, σ_{ij} the inplane stress components, $C_{11}=\lambda+2\mu$ and $C_{12}=\lambda$, and λ and μ denoting Lame's constant and the shear modulus at $\boldsymbol{X}$=0 respectively. If the deformation is plane strain, the displacements $\boldsymbol{u}$ and $\boldsymbol{v}$ which are derived from dilatational and shear wave potentials $\boldsymbol{\Phi}$ and $\boldsymbol{\Psi}$ can be expressed by Eq. (2)

$$\boldsymbol{u}=\frac{\partial\boldsymbol{\Phi}}{\partial\boldsymbol{X}}+\frac{\partial\boldsymbol{\Psi}}{\partial\boldsymbol{Y}},\quad \boldsymbol{v}=\frac{\partial\boldsymbol{\Phi}}{\partial\boldsymbol{Y}}-\frac{\partial\boldsymbol{\Psi}}{\partial\boldsymbol{X}} \tag{2}$$

The equilibrium in the transient dynamic state is given by Eq. (3)

$$\begin{aligned}&\frac{\partial\sigma_{XX}}{\partial X}+\frac{\partial\tau_{XY}}{\partial Y}=\rho\frac{\partial^2 u}{\partial t^2},\\ &\frac{\partial\tau_{XY}}{\partial X}+\frac{\partial\sigma_{YY}}{\partial Y}=\rho\frac{\partial^2 v}{\partial t^2}\end{aligned} \tag{3}$$

Substituting Eq. (2) into Eq. (1), and substituting Eq. (1) into Eq. (3), the equations for the dynamic state can be obtained as

$$\begin{aligned}&\left[C_{11}\left(\frac{\partial^3\Phi}{\partial X^3}+\frac{\partial^3\Psi}{\partial X^2\partial Y}\right)+C_{12}\left(\frac{\partial^3\Phi}{\partial X\partial Y^2}-\frac{\partial^3\Psi}{\partial X^2\partial Y}\right)+\right.\\ &\left.C_{66}\left(2\frac{\partial^3\Phi}{\partial X\partial Y^2}+\frac{\partial^3\Psi}{\partial Y^3}-\frac{\partial^3\Psi}{\partial X^2\partial Y}\right)\right]=\rho\frac{\partial^2}{\partial t^2}\left(\frac{\partial\Phi}{\partial X}+\frac{\partial\Psi}{\partial Y}\right)\end{aligned} \tag{4-a}$$

$$\begin{aligned}&\left[C_{22}\left(\frac{\partial^3\Phi}{\partial Y^3}-\frac{\partial^3\Psi}{\partial X\partial Y^2}\right)+C_{21}\left(\frac{\partial^3\Phi}{\partial X^2\partial Y}+\frac{\partial^3\Psi}{\partial X\partial Y^2}\right)+\right.\\ &\left.-C_{66}\left(2\frac{\partial^3\Phi}{\partial X^2\partial Y}-\frac{\partial^3\Psi}{\partial X^3}+\frac{\partial^3\Psi}{\partial X\partial Y^2}\right)\right]=\rho\frac{\partial^2}{\partial t^2}\left(\frac{\partial\Phi}{\partial Y}-\frac{\partial\Psi}{\partial X}\right)\end{aligned} \tag{4-b}$$

The moving crack tip coordinates are $x=X-a(t)$, $\boldsymbol{y}=\boldsymbol{Y}$. When Φ and Ψ have

function of position (x, y), crack tip speed $c(t)$ and time t at crack tip, the transformations for the transiently moving crack tip are given as

$$\frac{\partial^2}{\partial X^2}=\frac{\partial^2}{\partial x^2},\ \frac{\partial^2}{\partial Y^2}=\frac{\partial^2}{\partial y^2},$$
$$\frac{\partial^2}{\partial t^2}=c^2\frac{\partial^2}{\partial x^2}-2c\frac{\partial^2}{\partial x\partial t}-\dot{c}\frac{\partial}{\partial x}+\frac{\partial^2}{\partial t^2} \quad (5)$$

where $\dot{c}=\partial c/\partial t$ and $a(t)$ is the half crack length in center crack or the crack length of an edge crack. If the crack propagates at a constant velocity in steady state, $\partial^2/\partial t^2=c^2(\partial^2/\partial x^2)$. From the relations in Eq. (5), Eq. (4) is transformed as

$$\alpha_l^2\frac{\partial^2\Phi}{\partial x^2}+\frac{\partial^2\Phi}{\partial y^2}+\frac{\rho_o}{\mu_o(k+2)}(\dot{c}\frac{\partial\Phi}{\partial x}+2c\frac{\partial^2\Phi}{\partial x\partial t}-\frac{\partial^2\Phi}{\partial t^2})=0 \quad (6\text{-a})$$

$$\alpha_s^2\frac{\partial^2\Psi}{\partial x^2}+\frac{\partial^2\Psi}{\partial y^2}+\frac{\rho_o}{\mu_o}(\dot{c}\frac{\partial\Psi}{\partial x}+2c\frac{\partial^2\Psi}{\partial x\partial t}-\frac{\partial^2\Psi}{\partial t^2})=0 \quad (6\text{-b})$$

where $\alpha_l=\sqrt{1-(\frac{c}{c_l})^2}$, $\alpha_s=\sqrt{1-(\frac{c}{c_s})^2}$, $c_s=\sqrt{\frac{\mu}{\rho}}$ $c_l=c_s\sqrt{\frac{2(1-\nu)}{1-2\nu}}$ for plane strain, $c_l=c_s\sqrt{\frac{2}{1-\nu}}$ for plane stress

c, c_l and c_s are the crack propagation velocity, elastic dilatational wave velocity and elastic shear wave velocity at the crack tip. It is very difficult to obtain analytical solutions for the elastodynamic differential equation (6). Thus, an asymptotic expansion analysis of stress and displacement fields around the propagating crack is employed. To obtain an asymptotic expansion of the fields around the crack tip, we assume the general solutions of Eq. (6) for Φ and Ψ as follows

$$\Phi(z_l,t)=-\mathrm{Re}\int\phi_n(z_l,t)dz_l,$$
$$\Psi(z_s,t)=-\mathrm{Im}\int\psi_n(z_s,t)dz_s \quad (7)$$

$\phi_n(z_l)$ and $\psi_n(z_l)$ can be written with a power series as

$$\phi_n(z_l,t)=\sum_{n=1}^{n}A_n(t)z_l^{n/2},$$
$$\psi_n(z_s,t)=\sum_{n=1}^{n}B_n(t)z_s^{n/2} \quad (8)$$

where $A_n(t)=A_n^o(t)+iA_n^*(t)$ and $B_n(t)=B_n^o(t)+iB_n^*(t)$ and $z_{l,s}=x+m_{l,s}y$.

Substituting Eq (8) into Eq. (7) and substituting Eq (7) into Eq. (6-a), the structure for complex constant A_n of Eq. (6-a) become as Eq.(9)

$$\mathrm{Re}\left\{\frac{n}{2}(\alpha_l^2+m_l^2)A_nz_l^{n/2-1}\right\}=0:n=1,\ 2 \quad (9\text{-a})$$

$$\mathrm{Re}\left\{\frac{n}{2}(\alpha_l^2+m_l^2)A_nz_l^{n/2-1}=-\frac{2c^{1/2}}{c_l^2}\frac{\partial}{\partial t}\left(c^{1/2}A_{n-2}z_l^{n/2-1}\right)\right\}$$
$$:n=3,\ 4 \quad (9\text{-b})$$

$$\mathrm{Re}\left\{\frac{n}{2}(\alpha_l^2+m_l^2)A_nz_l^{n/2-1}=-\frac{2c^{1/2}}{c_l^2}\frac{\partial}{\partial t}\left(c^{1/2}A_{n-2}z_l^{n/2-1}\right)\right.$$
$$\left.+\frac{2}{n-2}\left[\frac{1}{c_l^2}\frac{\partial^2}{\partial t^2}\left(A_{n-4}z_l^{n/2-1}\right)\right]\right\}$$
$$:\ n=5,\ 6 \quad (9\text{-c})$$

When $n=1,\ 2$, $m_l=i\alpha_l^2$, and m_l is dependent on crack propagation velocity, physical properties and time. However, when $n\geq 3$, m_l is dependent on the crack propagation, physical properties and acceleration, and the value is changed for each n. The structure for the complex constants A_n and B_n can be written as

$$\mathrm{Re}\left\{\frac{n}{2}(\alpha_l^2+m_l^2)A_nz_l^{n/2-1}=-\frac{2c^{1/2}}{c_l^2}\frac{\partial}{\partial t}\left(c^{1/2}A_{n-2}z_l^{n/2-1}\right)+\right.$$
$$\left.\cdot\frac{2}{n-2}\left[\frac{1}{c_l^2}\frac{\partial^2}{\partial t^2}\left(A_{n-4}z_l^{n/2-1}\right)\right]\right\} \quad (10\text{-a})$$

$$\mathrm{Im}\left\{\frac{n}{2}(\alpha_s^2+m_s^2)B_nz_s^{n/2-1}=-\frac{2c^{1/2}}{c_s^2}\frac{\partial}{\partial t}\left(c^{1/2}B_{n-2}z_s^{n/2-1}\right)+\right.$$
$$\left.\cdot\frac{2}{n-2}\left[\frac{1}{c_s^2}\frac{\partial^2}{\partial t^2}\left(B_{n-4}z_s^{n/2-1}\right)\right]\right\} \quad (10\text{-b})$$

where $n\leq 0$ then A_n and $B_n=0$.

Thus, when Φ and Ψ in Eq. (6) can be expanded by powers as Eq. (8), the structure of Eq. (6) can be expressed as Eq. (11)

$$\alpha_l^2\frac{\partial^2\Phi_n}{\partial x^2}+\frac{\partial^2\Phi_n}{\partial y^2}=-\frac{2c^{1/2}}{c_l^2}\frac{\partial}{\partial t}\left(c^{1/2}\frac{\partial\Phi_{n-2}}{\partial x}\right)+\frac{1}{c_l^2}\frac{\partial^2\Phi_{n-4}}{\partial t^2} \quad (11\text{-a})$$

$$\alpha_s^2 \frac{\partial^2 \Psi_n}{\partial x^2} + \frac{\partial^2 \Psi_n}{\partial y^2} = -\frac{2c^{1/2}}{c_s^2} \frac{\partial}{\partial t}\left(c^{1/2} \frac{\partial \Psi_{n-2}}{\partial x} \right) + \frac{1}{c_s^2} \frac{\partial^2 \Psi_{n-4}}{\partial t^2} \tag{11-b}$$

where $n \le 0$, then $\Phi_n = \Psi_n = 0$

2.2. Stress and displacement fields for n = 1 , 2

When $n = 1,\ 2$, Eq. (11) is given as

$$\alpha_l^2 \frac{\partial^2 \Phi_n}{\partial x^2} + \frac{\partial^2 \Phi_n}{\partial y^2} = 0 \tag{12-a}$$

$$\alpha_s^2 \frac{\partial^2 \Psi_n}{\partial x^2} + \frac{\partial^2 \Psi_n}{\partial y^2} = 0 \tag{12-b}$$

Eqs (12-a) and (12-b) are the Laplace's equation in complex domain $z_{l(s)} = x + m_{l(s)} y$ and the same as that for steady state and can be rewritten as $(\alpha_l^2 + m_l^2)\Phi_n''(z_l, t) = 0$ and $(\alpha_s^2 + m_s^2)\Psi_n''(z_s, t) = 0$. Thus $m_l = i\alpha_l$ and $m_s = i\alpha_s$. Substituting the differentiation of Φ_n and Ψ_n in Eq. (7) into Eq. (2), the displacements $\boldsymbol{u}$ and $\boldsymbol{v}$ for $\boldsymbol{n}$ = 1 and 2 can be expressed as Eq. (13).

$$\begin{aligned} u &= -\mathrm{Re}\{\phi_n(z_l, t) + \alpha_s \psi_n(z_s, t)\} \\ v &= \mathrm{Im}\{\alpha_l \phi_n(z_l, t) + \psi_n(z_s, t)\} \end{aligned} \tag{13}$$

Substituting the differentiation of Eq. (13) into Eq. (1), the stress σ_{ij} for $\boldsymbol{n}$ = 1 and 2 can be expressed as Eq. (14).

$$\begin{aligned} \sigma_{xx} &= -\mu\,\mathrm{Re}\{(1 + 2\alpha_l^2 - \alpha_s^2)\phi_n'(z_l, t) + 2\alpha_s \psi_n'(z_s, t)\} \\ \sigma_{yy} &= \mu\,\mathrm{Re}\{(1 + \alpha_s^2)\phi_n'(z_l, t) + 2\alpha_s \psi_n'(z_s, t)\} \\ \tau_{xy} &= \mu\,\mathrm{Im}\{2\alpha_l \phi_n'(z_l, t) + (1 + \alpha_s^2)\psi_n'(z_s, t)\} \end{aligned} \tag{14}$$

Subsituting Eq. (7) into Eq. (14), applying traction free boundary conditions to the crack surface, A_n and B_n can be obtained as

$$\begin{aligned} A_n^o(t) &= -\frac{2}{\mu\sqrt{2\pi}} B_I(c) K_n^o(t), \quad A_n^*(t) = \frac{2}{\mu\sqrt{2\pi}} B_{II}(c) K_n^*(t) \\ B_n^o(t) &= \frac{2}{\mu\sqrt{2\pi}} h_n^0 B_I(c) K_n^o(t), \\ B_n^*(t) &= -\frac{2}{\mu\sqrt{2\pi}} h_n^* B_{II}(c) K_n^*(t) \end{aligned} \tag{15}$$

where

$$h_1^o = h_2^* = \frac{2\alpha_l}{1 + \alpha_s^2}, \quad h_1^* = h_2^o = \frac{1 + \alpha_s^2}{2\alpha_s}$$

$$B_I(c) = \frac{1 + \alpha_s^2}{4\alpha_l \alpha_s - (1 + \alpha_s^2)^2},$$

$$B_{II}(c) = \frac{2\alpha_s}{4\alpha_l \alpha_s - (1 + \alpha_s^2)^2}$$

K_1^o and K_1^* for $\boldsymbol{n} = 1$ are the stress intensity factors $K_I^d(t)$ and $K_{II}^d(t)$ respectively.

Thus, the stresses for a propagating crack can be obtained as Eq. (16).

$$\begin{aligned} \sigma_{xxn} &= \frac{K_n^o B_I(c)}{\sqrt{2\pi}} n\Big\{(1 + 2\alpha_l^2 - \alpha_s^2) r_l^{\frac{n-2}{2}} \cos(\frac{n-2}{2})\theta_l \\ &\quad - 2\alpha_s h_n^o r_s^{\frac{n-2}{2}} \cos(\frac{n-2}{2})\theta_s \Big\} \\ &\quad + \frac{K_n^* B_{II}(c)}{\sqrt{2\pi}} n\Big\{(1 + 2\alpha_l^2 - \alpha_s^2) r_l^{\frac{n-2}{2}} \sin(\frac{n-2}{2})\theta_l \\ &\quad - 2\alpha_s h_n^* r_s^{\frac{n-2}{2}} \sin(\frac{n-2}{2})\theta_s \Big\} \\ \sigma_{yyn} &= \frac{K_n^o B_I(c)}{\sqrt{2\pi}} n\Big\{-(1 + \alpha_s^2) r_l^{\frac{n-2}{2}} \cos(\frac{n-2}{2})\theta_l \\ &\quad + 2\alpha_s h_n^o r_s^{\frac{n-2}{2}} \cos(\frac{n-2}{2})\theta_s \Big\} \\ &\quad + \frac{K_n^* B_{II}(c)}{\sqrt{2\pi}} n\Big\{-(1 + \alpha_s^2) r_l^{\frac{n-2}{2}} \sin(\frac{n-2}{2})\theta_l \\ &\quad + 2\alpha_s h_n^* r_s^{\frac{n-2}{2}} \sin(\frac{n-2}{2})\theta_s \Big\} \\ \tau_{xyn} &= \frac{K_n^o B_I(c)}{\sqrt{2\pi}} n\Big\{-2\alpha_l r_l^{\frac{n-2}{2}} \sin(\frac{n-2}{2})\theta_l \\ &\quad + (1 + \alpha_s^2) h_n^o r_s^{\frac{n-2}{2}} \sin(\frac{n-2}{2})\theta_s \Big\} \\ &\quad + \frac{K_n^* B_{II}(c)}{\sqrt{2\pi}} n\Big\{2\alpha_l r_l^{\frac{n-2}{2}} \cos(\frac{n-2}{2})\theta_l \\ &\quad - (1 + \alpha_s^2) h_n^* r_s^{\frac{n-2}{2}} \cos(\frac{n-2}{2})\theta_s \Big\} \end{aligned} \tag{16}$$

The displacement for a propagating crack can be

obtained as Eq. (17).

$$u_n = \frac{K_n^o B_I(c)}{\mu}\sqrt{\frac{2}{\pi}}\left\{r_l^{\frac{n}{2}}\cos(\frac{n}{2})\theta_l - \alpha_s h_n^o r_s^{\frac{n}{2}}\cos(\frac{n}{2})\theta_s\right\}$$
$$+\frac{K_n^* B_{II}(c)}{\mu}\sqrt{\frac{2}{\pi}}\left\{r_l^{\frac{n}{2}}\sin(\frac{n}{2})\theta_l - \alpha_s h_n^* r_s^{\frac{n}{2}}\sin(\frac{n}{2})\theta_s\right\}$$
$$v_n = \frac{K_n^o B_I(c)}{\mu}\sqrt{\frac{2}{\pi}}\left\{-\alpha_l r_l^{\frac{n}{2}}\sin(\frac{n}{2})\theta_l + h_n^o r_s^{\frac{n}{2}}\sin(\frac{n}{2})\theta_s\right\}$$
$$+\frac{K_n^* B_{II}(c)}{\mu}\sqrt{\frac{2}{\pi}}\left\{\alpha_l r_l^{\frac{n}{2}}\cos(\frac{n}{2})\theta_l - h_n^* r_s^{\frac{n}{2}}\cos(\frac{n}{2})\theta_s\right\} \quad (17)$$

$$\boldsymbol{r_j} = \sqrt{\boldsymbol{x}^2 + (\alpha_j \boldsymbol{y})^2},\ \ \theta_j = \tan^{-1}(\alpha_j \boldsymbol{y}/\boldsymbol{x}),\ \ \boldsymbol{j} = \boldsymbol{l}, \boldsymbol{s}$$

2.3. Stress and displacement fields for n =3

From Eq. (10), the m_l and m_s can be obtained as follows

$$m_l = i\hat{\alpha}_l,\ \ m_s = i\hat{\alpha}_s \quad (18)$$

For mode I state ;

$$\hat{\alpha}_l = \sqrt{\alpha_l^2 + k_1\frac{2}{3}\frac{c}{c_l^2}\left(\frac{\dot{c}}{c} + 2\frac{\dot{A}_1^o}{A_1^o} + \frac{2\dot{\alpha}_l}{\alpha_l}\sin^2\frac{\theta_l}{2}\right)},$$
$$\hat{\alpha}_s = \sqrt{\alpha_s^2 + k_1\frac{2}{3}\frac{c}{c_s^2}\left(\frac{\dot{c}}{c} + 2\frac{\dot{B}_1^o}{B_1^o} + \frac{2\dot{\alpha}_s}{\alpha_s}\cos^2\frac{\theta_s}{2}\right)}$$
$$k_1 = A_1^o / A_3^o = B_1^o / B_3^o,$$
$$\dot{A}_1^o = -\frac{2}{\mu\sqrt{2\pi}}\left[\frac{2\alpha_s\dot{\alpha}_s D - (1+\alpha_s^2)\dot{D}}{D^2}K_I^d + \frac{1+\alpha_s^2}{D}\dot{K}_I^d\right],$$
$$\dot{B}_1^o = \frac{2}{\mu\sqrt{2\pi}}\left[\frac{2\dot{\alpha}_l D - 2\alpha_l\dot{D}}{D^2}K_I^d + \frac{2\alpha_l}{D}\dot{K}_I^d\right],$$
$$D = 4\alpha_l\alpha_s - (1+\alpha_s^2)^2,$$
$$\dot{D} = -4c\dot{c}\left[\frac{\alpha_s}{\alpha_l c_l^2} + \frac{\alpha_l}{\alpha_s c_s^2} - \frac{1+\alpha_s^2}{c_s^2}\right]$$

For mode II state ;

$$\hat{\alpha}_l = \sqrt{\alpha_l^2 + k_2\frac{2}{3}\frac{c}{c_l^2}\left(\frac{\dot{c}}{c} + 2\frac{\dot{A}_1^*}{A_1^*} + \frac{2\dot{\alpha}_l}{\alpha_l}\cos^2\frac{\theta_l}{2}\right)},$$
$$\hat{\alpha}_s = \sqrt{\alpha_s^2 + k_2\frac{2}{3}\frac{c}{c_s^2}\left(\frac{\dot{c}}{c} + 2\frac{\dot{B}_1^*}{B_1^*} + \frac{2\dot{\alpha}_s}{\alpha_s}\sin^2\frac{\theta_s}{2}\right)}$$
$$k_2 = A_1^* / A_3^* = B_1^* / B_3^*,$$
$$\dot{A}_1^* = \frac{2}{\mu\sqrt{2\pi}}\left[\frac{2\dot{\alpha}_s D - 2\alpha_s\dot{D}}{D^2}K_{II}^d + \frac{2\alpha_s}{D}\dot{K}_{II}^d\right],$$
$$\dot{B}_1^* = -\frac{2}{\mu\sqrt{2\pi}}\left[\frac{2\alpha_s\dot{\alpha}_s D - (1+\alpha_s^2)\dot{D}}{D^2}K_{II}^d + \frac{1+\alpha_s^2}{D}\dot{K}_{II}^d\right],$$
$$\dot{c} = dc/dt,\ \ \dot{\alpha}_s = \frac{-c\dot{c}}{\alpha_s c_s^2}\ \ \dot{\alpha}_l = \frac{-c\dot{c}}{\alpha_l c_l^2},$$
$$\dot{K}_{I(II)}^d = dK_{I(II)}/dt$$

$m_j(=i\hat{\alpha}_j)$ in Eq. (18) is dependent on crack propagation velocity (c), acceleration ($\dot{c}$), rate of change of the stress intensity factor ($\dot{K}$), physical properties (c_l, c_s) and angle (θ) at the crack tip. The limit of the accelerations can be obtained from Eq. (18) under K_j, K_I^d, $\dot{K}$, c, c_l and c_s. The unit of k_1 and k_2 is the length (m). The value of the last term which is related to θ in $\hat{\alpha}_j (j = l, s)$ is very small, compared to the other terms. Figure 1 show $m_j(\theta) / m_j(c)$, in which $m_j(c)$ is the term excluding the last term related to θ in $\hat{\alpha}_j$. As shown in Fig. 1, $m_j(\theta) / m_j(c)$ approaches one. This indicates that the value of the last terms related to θ is very small compared to one of the other terms. Thus, we can assume that m_j is independent of x and y, and it simplifies the problem. When m_l and m_s are the same as Eq. (18), Eq. (11) can expressed as Eq. (19)

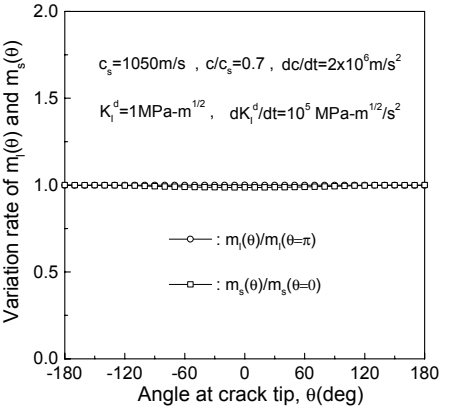

Fig. 1. Variation in the rate of $m_l(\theta)$ and $m_s(\theta)$ with angle at crack tip for $k_1 > 0.1$.

$$\hat{\alpha}_l^2 \frac{\partial^2 \Phi_3(\hat{z}_l,t)}{\partial x^2} + \frac{\partial^2 \Phi_3(\hat{z}_l,t)}{\partial y^2} = 0,$$
$$\hat{\alpha}_s^2 \frac{\partial^2 \Psi_3(\hat{z}_s,t)}{\partial x^2} + \frac{\partial^2 \Psi_3(\hat{z}_s,t)}{\partial y^2} = 0 \quad (19)$$

where $\hat{z}_j = x + i\hat{\alpha}_j y$ and $\hat{\alpha}_j$ is dependent on a transient factors in addition to physical properties and crack propagation velocity. Eq. (19) is also the Laplace's equation in complex domain $\hat{z}_j$ and can be rewritten as $(\hat{\alpha}_l^2 + m_l^2)\Phi_n''(\hat{z}_l,t) = 0$ and $(\hat{\alpha}_s^2 + m_s^2)\Psi_n''(\hat{z}_s,t) = 0$. Thus $m_l = i\hat{\alpha}_l$ and $m_s = i\hat{\alpha}_s$. When $n > 3$, Laplace's equations for Φ_n and Ψ_n can be also obtained and the solutions of the Laplace's equations have harmonic functions. Thus, $\Phi_3(\hat{z}_l,t)$ and $\Psi_3(\hat{z}_l,t)$ can be written as

$$\Phi_3(\hat{z}_l,t) = -\mathrm{Re}\int \phi_3(\hat{z}_l,t)d\hat{z}_l$$
$$\Psi_3(\hat{z}_s,t) = -\mathrm{Im}\int \psi_3(\hat{z}_s,t)d\hat{z}_s \quad (20)$$

where $\hat{z}_j = x + \hat{m}_j = x + i\hat{\alpha}_j y$

$\hat{r}_j = \sqrt{x^2 + (\hat{\alpha}_j y)^2}$, $\hat{\theta}_j = \tan^{-1}[\hat{\alpha}_j y / x]$, $\quad j = l, s$

The $\phi_3(\hat{z}_l,t)$ and $\psi_3(\hat{z}_s,t)$ are dependent on acceleration(dc/dt) and the rate of change of the stress intensity factor (dK/dt) in addition to the crack propagation velocity and physical properties. Substituting the differentiation of $\Phi_3(\hat{z}_l,t)$ and $\Psi_3(\hat{z}_s,t)$ in Eq. (20) into Eq. (2), the displacements u and v for $n = 3$ can be expressed as Eq. (21).

$$u = -\mathrm{Re}\{\phi_3(\hat{z}_l,t) + \hat{\alpha}_s\psi_3(\hat{z}_s,t)\},$$
$$v = \mathrm{Im}\{\hat{\alpha}_l\phi_n(\hat{z}_l,t) + \psi_n(\hat{z}_s,t)\} \quad (21)$$

Substituting the differentiation of Eq. (21) into Eq. (1), the stress σ_{ij} for $n = 3$ can be expressed as Eq. (22).

$$\sigma_{xx} = -\mu\mathrm{Re}\left\{\left[\frac{1-\alpha_s^2}{1-\alpha_l^2}(1-\hat{\alpha}_l^2) + 2\hat{\alpha}_l^2\right]\phi_3'(\hat{z}_l,t) + 2\hat{\alpha}_s\psi_3'(\hat{z}_s,t)\right\}$$
$$\sigma_{yy} = \mu\mathrm{Re}\left\{\left[-\frac{1-\alpha_s^2}{1-\alpha_l^2}(1-\hat{\alpha}_l^2) + 2\right]\phi_3'(\hat{z}_l,t) + 2\hat{\alpha}_s\psi_3'(\hat{z}_s,t)\right\}$$
$$\tau_{xy} = \mu\,\mathrm{Im}\{2\hat{\alpha}_l\phi_3'(\hat{z}_l,t) + (1+\hat{\alpha}_s^2)\psi_3'(\hat{z}_s,t)\} \quad (22)$$

$\phi_3(\hat{z}_l,t)$ and $\psi_3(\hat{z}_s,t)$ can be written as

$$\phi_3(\hat{z}_l,t) = [A_3^o(t) + iA_3^*(t)]\hat{z}_l^{3/2}$$
$$\psi_3(\hat{z}_s,t) = [B_3^o(t) + iB_3^*(t)]\hat{z}_s^{3/2} \quad (23)$$

Substituting Eq. (23) into Eq. (22), the stress fields become

$$\sigma_{xx3} = -\mu\frac{3}{2}\left\{A_3^o\left[\frac{1-\alpha_s^2}{1-\alpha_l^2}(1-\hat{\alpha}_l^2) + 2\hat{\alpha}_l^2\right]\hat{r}_l^{1/2}\cos\frac{\hat{\theta}_l}{2} + 2B_3^o\hat{\alpha}_s\hat{r}_s^{1/2}\cos\frac{\hat{\theta}_s}{2}\right\}$$
$$+\mu\frac{3}{2}\left\{A_3^*\left[\frac{1-\alpha_s^2}{1-\alpha_l^2}(1-\hat{\alpha}_l^2) + 2\hat{\alpha}_l^2\right]\hat{r}_l^{1/2}\sin\frac{\hat{\theta}_l}{2} + 2B_3^*\hat{\alpha}_s\hat{r}_s^{1/2}\sin\frac{\hat{\theta}_s}{2}\right\}$$
$$\sigma_{yy3} = \mu\frac{3}{2}\left\{A_3^o\left[-\frac{1-\alpha_s^2}{1-\alpha_l^2}(1-\hat{\alpha}_l^2) + 2\right]\hat{r}_l^{1/2}\cos\frac{\hat{\theta}_l}{2} + 2B_3^o\hat{\alpha}_s\hat{r}_s^{1/2}\cos\frac{\hat{\theta}_s}{2}\right\}$$
$$-\mu\frac{3}{2}\left\{A_3^*\left[-\frac{1-\alpha_s^2}{1-\alpha_l^2}(1-\hat{\alpha}_l^2) + 2\right]\hat{r}_l^{1/2}\sin\frac{\hat{\theta}_l}{2} + 2B_3^*\hat{\alpha}_s\hat{r}_s^{1/2}\sin\frac{\hat{\theta}_s}{2}\right\}$$
$$\tau_{xy3} = \mu\frac{3}{2}\left\{A_3^o(2\hat{\alpha}_l)\hat{r}_l^{1/2}\sin\frac{\hat{\theta}_l}{2} + B_3^o(1+\hat{\alpha}_s^2)\hat{r}_s^{1/2}\sin\frac{\hat{\theta}_s}{2}\right\}$$
$$+\mu\frac{3}{2}\left\{A_3^*(2\hat{\alpha}_l)\hat{r}_l^{1/2}\cos\frac{\hat{\theta}_l}{2} + B_3^*(1+\hat{\alpha}_s^2)\hat{r}_s^{1/2}\cos\frac{\hat{\theta}_s}{2}\right\} \quad (24)$$

Applying traction free boundary conditions on the crack surface, A_3^o, B_3^o, A_3^* and B_3^* can be obtained as

$$A_3^o(t) = -\frac{2}{\mu_c\sqrt{2\pi}}\hat{B}_I(c,\dot{c},t)K_3^o(t),$$
$$A_3^*(t) = \frac{2}{\mu_c\sqrt{2\pi}}\hat{B}_{II}(c,\dot{c},t)K_3^*(t),$$
$$B_3^o(t) = -h_3^o(c,\dot{c},t)A_3^o(t),$$
$$B_3^*(t) = -h_3^*(c,\dot{c},t)A_3^*(t) \quad (25)$$

where

$$\hat{B}_I(c,\dot{c},t)=\frac{(1+\hat{\alpha}_s^2)(1-\alpha_I^2)}{4\alpha_I\hat{\alpha}_s(1-\alpha_I^2)+(1+\alpha_s^2)[(1-\alpha_s^2)(1-\hat{\alpha}_I^2)-2(1-\alpha_I^2)]},$$

$$\hat{B}_{II}(c,\dot{c},t)=\frac{2\hat{\alpha}_s(1-\alpha_I^2)}{4\alpha_I\hat{\alpha}_s(1-\alpha_I^2)+(1+\alpha_s^2)[(1-\alpha_s^2)(1-\hat{\alpha}_I^2)-2(1-\alpha_I^2)]},$$

$$h_3^o(c,\dot{c},t)=\frac{2\hat{\alpha}_I}{(1+\hat{\alpha}_s^2)},$$

$$h_3^*(c,\dot{c},t)=\frac{2(1-\alpha_I^2)-(1-\alpha_s^2)(1-\hat{\alpha}_I^2)}{2\hat{\alpha}_s(1-\alpha_I^2)}$$

Substituting Eq. (25) into Eq. (24), applying $A_3^o=A_1^o/k_1$ and $A_3^*=A_1^*/k_2$, the stress fields σ_{ij3} can be obtained as Eq. (26)

$$\sigma_{xx3}=\frac{3K_I^d}{k_1\sqrt{2\pi}}B_I(c)\left\{\left[\frac{1-\alpha_s^2}{1-\alpha_I^2}(1-\hat{\alpha}_I^2)+2\hat{\alpha}_I^2\right]\hat{r}_I^{1/2}\cos\frac{\hat{\theta}_I}{2}-2h_3^o\hat{\alpha}_s\hat{r}_s^{1/2}\cos\frac{\hat{\theta}_s}{2}\right\}$$
$$+\frac{3K_{II}^d}{k_2\sqrt{2\pi}}B_{II}(c)\left\{\left[\frac{1-\alpha_s^2}{1-\alpha_I^2}(1-\hat{\alpha}_I^2)+2\hat{\alpha}_I^2\right]\hat{r}_I^{1/2}\sin\frac{\hat{\theta}_I}{2}-2h_3^*\hat{\alpha}_s\hat{r}_s^{1/2}\sin\frac{\hat{\theta}_s}{2}\right\}$$

$$\sigma_{yy3}=\frac{3K_I^d}{k_1\sqrt{2\pi}}B_I(c)\left\{\left[\frac{1-\alpha_s^2}{1-\alpha_I^2}(1-\hat{\alpha}_I^2)-2\right]\hat{r}_I^{1/2}\cos\frac{\hat{\theta}_I}{2}+2h_3^o\hat{\alpha}_s\hat{r}_s^{1/2}\cos\frac{\hat{\theta}_s}{2}\right\}$$
$$+\frac{3K_{II}^d}{k_2\sqrt{2\pi}}B_{II}(c)\left\{\left[\frac{1-\alpha_s^2}{1-\alpha_I^2}(1-\hat{\alpha}_I^2)-2\right]\hat{r}_I^{1/2}\sin\frac{\hat{\theta}_I}{2}+2h_3^*\hat{\alpha}_s\hat{r}_s^{1/2}\sin\frac{\hat{\theta}_s}{2}\right\}$$

$$\tau_{xy3}=\frac{3K_I^d}{k_1\sqrt{2\pi}}B_I(c)\left\{-2\hat{\alpha}_I\hat{r}_I^{1/2}\sin(\frac{\hat{\theta}_I}{2})+(1+\hat{\alpha}_s^2)h_3^o\hat{r}_s^{1/2}\sin(\frac{\hat{\theta}_s}{2})\right\}$$
$$+\frac{3K_{II}^d}{k_2\sqrt{2\pi}}B_{II}(c)\left\{2\hat{\alpha}_I\hat{r}_I^{1/2}\cos(\frac{\hat{\theta}_I}{2})-(1+\hat{\alpha}_s^2)h_3^*\hat{r}_s^{1/2}\cos(\frac{\hat{\theta}_s}{2})\right\} \quad (26)$$

Substituting Eq. (23) into Eq.(21), the displacement fields can be obtained as

$$u_3=\frac{K_I^dB_I(c)}{k_1\mu}\sqrt{\frac{2}{\pi}}\left\{\hat{r}_I^{\frac{3}{2}}\cos(\frac{3}{2})\hat{\theta}_I-\hat{\alpha}_sh_3^or_s^{\frac{3}{2}}\cos(\frac{3}{2})\hat{\theta}_s\right\}$$
$$+\frac{K_{II}^dB_{II}(c)}{k_2\mu}\sqrt{\frac{2}{\pi}}\left\{\hat{r}_I^{\frac{3}{2}}\sin(\frac{3}{2})\hat{\theta}_I-\hat{\alpha}_sh_3^*\hat{r}_s^{\frac{3}{2}}\sin(\frac{3}{2})\hat{\theta}_s\right\}$$

$$v_3=\frac{K_I^dB_I(c)}{k_1\mu}\sqrt{\frac{2}{\pi}}\left\{-\hat{\alpha}_I\hat{r}_I^{\frac{3}{2}}\sin(\frac{3}{2})\hat{\theta}_I+h_3^o\hat{r}_s^{\frac{3}{2}}\sin(\frac{3}{2})\hat{\theta}_s\right\}$$
$$+\frac{K_{II}^dB_{II}(c)}{k_2\mu}\sqrt{\frac{2}{\pi}}\left\{\hat{\alpha}_I\hat{r}_I^{\frac{3}{2}}\cos(\frac{3}{2})\hat{\theta}_I-h_3^*\hat{r}_s^{\frac{3}{2}}\cos(\frac{3}{2})\hat{\theta}_s\right\} \quad (27)$$

Finally, the fields for a transient crack , σ_{ij} and u_j are given in Eq. (28)

$$\sigma_{ij}=\sum_{n=1}^{3}\sigma_{ijn},\quad u_j=\sum_{n=1}^{3}u_{jn} \quad (28)$$

Table 1. Mechanical properties.

Shear Modulus, μ	$\mu=1.316$ (GPa)
Material Fringe Constant, f	f = 15 (kN/m-fringe)
Poisson's ratio, ν	ν =0.38
Density, ρ	ρ =1200 (kg/m^3)

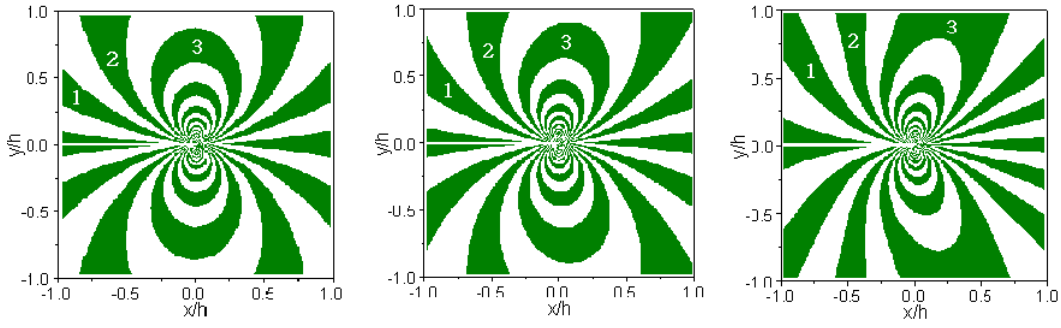

(a) $\dot{K}_I^d=0$ (b) $\dot{K}_I^d=100\text{MPa}\sqrt{\text{m}}/\text{s}^2$ (c) $\dot{K}_I^d=300\text{MPa}\sqrt{\text{m}}/\text{s}^2$

Fig. 2. Isochromatic fringe patterns obtained for a stationary crack tip (M=0.02) under $\dot{c}=0$, $K_I^d=1.0\text{MPa}\sqrt{\text{m}}$ and $k_1=1$.

The stress fields in Eq. (28) satisfy the traction free condition on the crack surface ($\theta = \pm\pi$). When the $\dot{c}$ and $\dot{K}$ are zero, the equations reduce to the fields for a steady state. It can be seen from the stress and displacement fields (equations 28) that the terms of n=1 and 2 are the same as those in the steady state and higher orders terms of $n \geq 3$ have terms of corresponding to the crack tip accelerations and the rate of change of stress intensity factor. Unlike the results reported by Freund (1990) and Rosakis et al. (1991), the higher order terms in this fields are not affected directly by the stress intensity factors and are not separated into two terms for stress intensity factors and non-stress intensity factors. This structure of these fields is general and universal.

Generally, in order to obtain fracture parameters for a steady state crack from experimental data obtained through optical techniques such as photoelasticity or coherent gradient sensing (CGS) the use of the first few terms of the stress fields is sufficient. However, in the case of an unsteady crack, it is necessary to use at least three terms for the fields to explicitly account for the transient effects when extracting fracture parameters from experimental data.

3. Discussion on solutions

3.1 Contours of constant maximum shear stress

In order to investigate the effects of the transient terms on a dynamic fracture, contours of constant maximum shear stress (isochromatics) are generated for the opening mode using the terms $n = 1$ and 3 in Eq. (28). The material thickness (h) used in generating the contours is 9.5 mm and the value of the material properties are shown in table 1. Isochromatics at each point around crack tip are generated by the stress optic law (Eq. 29) combined with stress fields.

$$\sqrt{(\sigma_{xx} - \sigma_{yy})^2 + 4\tau_{xy}^2} = \frac{Nf_\sigma}{h} \tag{29}$$

where N is the fringe order, h the plate thickness and f_σ the material fringe constant

In experiments (Ravi-Chandar, 1993), the rate of increase in the dynamic stress intensity factor, $\dot{K}_I^d$, ranges from 1.0MPa$\sqrt{\text{m}}$/s for quasi-static loading, resulting in a dynamic fracture to about the order of 10^5~10^8MPa$\sqrt{\text{m}}$/s at crack initiation. Arakawa et al. (2000) showed that the rate of change of velocity at the initiation of a single edge crack could be of the order of 5×10^5 m/s^2. Thus, the values of $\dot{K}_I^d$ and $\dot{c}$ are varied in this range for generating the contours and the remote stress in the x direction σ_{ox} was set to zero.

Figure 2 shows the effect of the rate of change of mode I stress intensity factor $\dot{K}_I^d$ for a stationary crack tip (M=0.02) in under $\dot{c} = 0$ and $k_1 = 1$, where M is c/c_s. When $\dot{K}_I^d = 0$, the fringes are upright. As $\dot{K}_I^d$ increases, the fringes tilt forward around the crack tip, and the size and number of fringes increases. This variation occurs largely when the rate of change of the stress intensity factor is high.

Figure 3 shows the effect of crack tip acceleration $\dot{c}$ for a crack tip propagating with M=0.5 under $\dot{K}_I^d = 0$ and $k_1 = 0.5$. When a crack velocity is low, a high rate of change of velocity in Eq. (18) can't be applied. However, a selecting the small value of

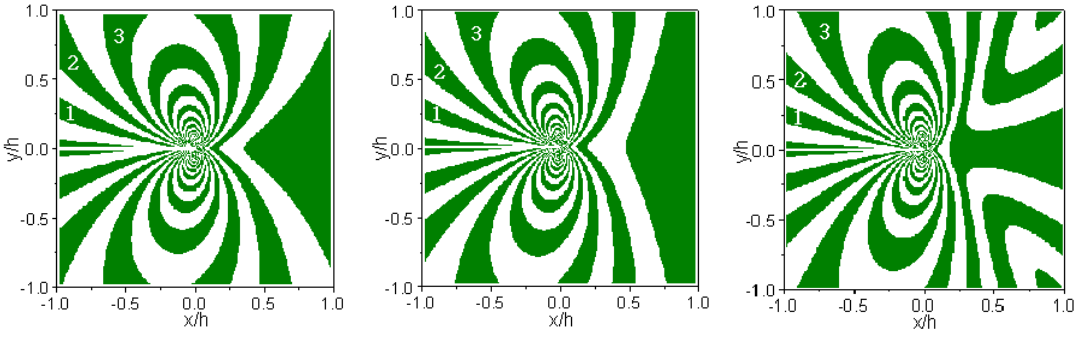

(a) $\dot{c} = 0$ (b) $\dot{c} = 4\times10^5$ m/s^2 (c) $\dot{c} = 8\times10^5$ m/s^2

Fig. 3. Isochromatic fringe patterns obtained for a crack tip propagating with M=0.5 under $\dot{K}_I^d = 0$, $K_I^d = 1.0\text{MPa}\sqrt{\text{m}}$ and $k_1 = 0.5$.

$k_1 (= A_1^o / A_3^o)$, a higher $\dot{c}$ can be applied in Eq. (18). It can be seen in Fig. 3 that the fringes tilt backward around the crack tip and their sizes increase with increasing crack tip acceleration. This variation also occurs largely at a high rate of change of velocity. Generally, isochromatic fringes for fast propagating cracks tilt more towards the crack face (backward) compared to those for a stationary crack. The phenomenon also occurs for a high crack tip acceleration $\dot{c}$.

Figure 4 shows the effect of crack tip acceleration $\dot{c}$ for a crack tip propagating with M=0.5 under, $\dot{K}_I^d = 10^5 \text{MPa}\sqrt{\text{m}}/\text{s}^2$ and $k_1 = 0.5$. Under $\dot{K}_I^d = 10^5 \text{MPa}\sqrt{\text{m}}/\text{s}^2$, it can be also observed that the fringes also tilt backward around the crack tip and their sizes increase as the crack tip acceleration increases. Compared with Fig. 3 and 4, as $\dot{K}_I^d$ increases as in Fig. 2, the fringes around the crack-tip tilt forward.

The above results indicate that the isochromatic fringes of mode I using the stress fields obtained in this study are symmetric about x axis under very rapid transient state and tilt backward around the crack tip with increasing crack tip acceleration $\dot{c}$ and tilt forward around the crack tip with increasing the rate of change of the dynamic mode I stress intensity factor $\dot{K}_I^d$.

3.2 Comparison with fields obtained by Rosakis et al. (1991)

Figure 5 shows the contours for constant maximum shear stress generated from fields obtained by Rosakis et al. (1991). Where, σ_{xx} and σ_{yy} among the three stress components can be written as follows.

$$\frac{\sigma_{xx}}{\mu} = \frac{K_I^d B_I(c)}{\mu\sqrt{2\pi}}\left\{(1+2\alpha_l^2-\alpha_s^2) r_l^{-\frac{1}{2}} \cos\frac{\theta_l}{2} - \frac{4\alpha_l\alpha_s}{1+\alpha_s^2} r_s^{-\frac{1}{2}} \cos\frac{\theta_s}{2}\right\} + 4(\alpha_l^2-\alpha_s^2) A_2(t)$$
$$+\frac{15}{4}\left\{(1+2\alpha_l^2-\alpha_s^2) r_l^{\frac{1}{2}} \cos\frac{\theta_l}{2} - \frac{4\alpha_l\alpha_s}{1+\alpha_s^2} r_s^{\frac{1}{2}} \cos\frac{\theta_s}{2}\right\} A_3(t)$$
$$+ D_l^1\{A_1(t)\}\left\{r_l^{1/2}\left[\frac{(1+\alpha_l^2)(\alpha_l^2-\alpha_s^2)+(1-\alpha_l^2)^2}{2(1-\alpha_l^2)}\cos\frac{\theta_l}{2} + \frac{1+2\alpha_l^2-\alpha_s^2}{8}\cos\frac{3\theta_l}{2}\right] - \frac{\alpha_l\alpha_s}{2(1+\alpha_s^2)} r_s^{1/2}\cos\frac{\theta_s}{2}\right\}$$
$$+\frac{B_l(t)}{2}\left\{r_l^{1/2}\left[\frac{(2\alpha_l^2-\alpha_s^2-1)\alpha_l^2}{1-\alpha_l^2}\cos\frac{\theta_l}{2} + \left(\frac{5(2\alpha_l^2-\alpha_s^2)}{8} - \frac{\alpha_l^2-\alpha_s^2}{1-\alpha_l^2} - \frac{3}{8}\right)\cos\frac{3\theta_l}{2} + \frac{1+2\alpha_l^2-\alpha_s^2}{16}\cos\frac{7\theta_l}{2}\right]\right.$$
$$\left. - \frac{11\alpha_l\alpha_s}{4(1+\alpha_s^2)} r_s^{1/2}\cos\frac{\theta_s}{2}\right\}$$
$$+\frac{1}{4}\alpha_s D_s^1\{B_1(t)\}\left[r_s^{1/2}\cos\frac{3\theta_s}{2} - \frac{5-3\alpha_s^2}{1+\alpha_s^2} r_s^{1/2}\cos\frac{\theta_s}{2}\right]$$
$$+\frac{\alpha_s}{2} B_s(t) r_s^{1/2}\left[\frac{13}{8}\cos\frac{\theta_s}{2} + \frac{1}{4}\cos\frac{3\theta_s}{2} + \frac{1}{8}\cos\frac{7\theta_s}{2}\right]$$

$$\frac{\sigma_{yy}}{\mu} = \frac{K_I^d(t) B_I(c)}{\mu\sqrt{2\pi}}\left\{-(1+\alpha_s^2) r_l^{-\frac{1}{2}}\cos\frac{\theta_l}{2} + \frac{4\alpha_l\alpha_s}{1+\alpha_s^2} r_s^{-\frac{1}{2}}\cos\frac{\theta_s}{2}\right\}$$

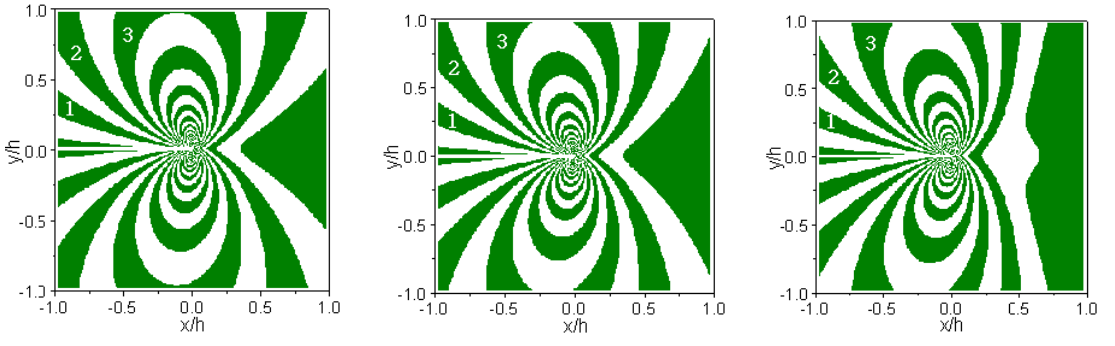

(a) $\dot{c} = 0$ (b) $\dot{c} = 5\times10^5 \text{m/s}^2$ (c) $\dot{c} = 1\times10^6 \text{m/s}^2$

Fig. 4. Isochromatic fringe patterns obtained for a crack tip propagating with M=0.5 under $\dot{K}_I^d = 10^5 \text{MPa}\sqrt{\text{m}}/\text{s}^2$, $K_I^d = 1.0\text{MPa}\sqrt{\text{m}}$ and $k_1 = 0.5$.

$$+\frac{15}{4}\left\{-(1+\alpha_s^2)r_l^{\frac{1}{2}}\cos\frac{\theta_l}{2}+\frac{4\alpha_l\alpha_s}{1+\alpha_s^2}r_s^{\frac{1}{2}}\cos\frac{\theta_s}{2}\right\}A_3(t)$$
$$+D_l^1\{A_1(t)\}\left\{r_l^{1/2}\left[\frac{(1+\alpha_l^2)(\alpha_l^2-\alpha_s^2)-(1-\alpha_l^2)^2}{2(1-\alpha_l^2)}\right.\right.$$
$$\left.\cos\frac{\theta_l}{2}-\frac{1+\alpha_s^2}{8}\cos\frac{3\theta_l}{2}\right]+\frac{\alpha_l\alpha_s}{2(1+\alpha_s^2)}r_s^{1/2}\cos\frac{\theta_s}{2}\Bigg\}$$
$$+\frac{1}{2}B_l(t)\left\{r_l^{1/2}\left[\frac{(1-\alpha_s^2)\alpha_l^2}{1-\alpha_l^2}\cos\frac{\theta_l}{2}\right.\right.$$
$$\left.\left(\frac{3-5\alpha_s^2}{8}-\frac{(\alpha_l^2-\alpha_s^2)}{1-\alpha_l^2}\right)\cos\frac{3\theta_l}{2}-\frac{1+\alpha_s^2}{16}\cos\frac{7\theta_l}{2}\right]$$
$$\left.+\frac{11\alpha_l\alpha_s}{4(1+\alpha_s^2)}r_s^{1/2}\cos\frac{\theta_s}{2}\right\}$$
$$-\frac{1}{4}\alpha_s D_s^1\{B_1(t)\}\left[r_s^{1/2}\cos\frac{3\theta_s}{2}-\frac{5-3\alpha_s^2}{1+\alpha_s^2}r_s^{1/2}\cos\frac{\theta_s}{2}\right]$$
$$-\frac{\alpha_s}{2}B_s(t)r_s^{1/2}\left[\frac{13}{8}\cos\frac{\theta_s}{2}+\frac{1}{4}\cos\frac{3\theta_s}{2}+\frac{1}{8}\cos\frac{7\theta_s}{2}\right] \quad (30)$$

where

$$D_l^1\{A_1(t)\}=-\frac{4\sqrt{c}}{\mu\sqrt{2\pi}\alpha_l^2c_l^2}\frac{d}{dt}\left\{\sqrt{c}B_I(c)K_I^d\right\},$$
$$D_s^1\{B_1(t)\}=\frac{4\sqrt{c}}{\mu\sqrt{2\pi}\alpha_s^2c_s^2}\frac{d}{dt}\left\{\sqrt{c}B_I(c)h(1)K_I^d\right\}$$
$$B_l(t)=\frac{2c^2}{\mu\sqrt{2\pi}\alpha_l^4c_l^4}B_I(c)K_I^d\frac{dc}{dt},$$
$$B_s(t)=-\frac{2c^2}{\mu\sqrt{2\pi}\alpha_s^4c_s^4}B_I(c)h(1)K_I^d\frac{dc}{dt}$$

As known in Fig. 5, the contours are not symmetric about the x axis except for the crack tip because their solutions can not have harmonic function. Actually, the fields very close to the crack tip don't explain effectively the transient effects. Thus, the stress components are not effective for analyzing a transient crack by photoelasticity. Even if the fields have some problems with respect to photoelasticity, the contours of the isopachic fringes on the constant first stress invariant ($\sigma_{xx}+\sigma_{yy}$) are the same as those in this study.

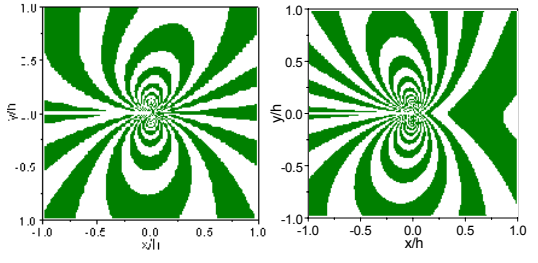

(a) (b)

Fig. 5. The Isochromatic fringe patterns generated from fields obtained by Rosakis et al. (1991) ; (a) is the same condition as Fig. 2(b); (b) is the same condition as Fig. 3(c).

3.3 Dynamic stress intensity factor during a crack acceleration and deceleration

Figure 6(a) shows the ratio of dynamic to static stress intensity factor versus normalized crack speed when a crack propagates with constant velocity or acc-eleration under the Rayleigh wave speed of $c_R=0.9235c_s$ in an infinite plate subjected to normal displacements on crack faces. The dynamic stress intensity factors can be obtained from assuming that the crack propagates with a constant y-displacement at a point on the crack surface away from the crack tip regardless of the crack speed, acceleration and deceleration. This crack propagation is quite possible in an infinite plate subjected to crack face pressure. Where K_I^s is a static stress intensity factor immediately prior to the crack propagation. To obtain the stress intensity factor in y-displacement component of Eq. (28), the following conditions were applied $\theta=\pi$, $r=0.01$ m and $k_1=0.5$. As known in Fig. 6 (a), the stress intensity factors decrease with increasing a crack speed, and they become zero when the crack velocity approaches the Rayleigh wave speed. Specially, the stress intensity factors increase rapidly when the crack propagates with high acceleration at a low velocity. However, the stress intensity factors are not almost affected by high acceleration at a high crack speed. When the crack propagates with a constant velocity, the normalized stress intensity factors are almost the same as those of the two self-similar central crack tips extending at same speed by crack face pressure (Freund, 1990). In an experiment using a single edge cracked tensile plate reported by Arakawa et al. (2000), the dynamic stress intensity factors increase as a crack propagates with acceleration, and decrease as a crack propagates with deceleration.

Figure 6 (b) shows the influence of the stress intensity factor on the rate of change of the mode I

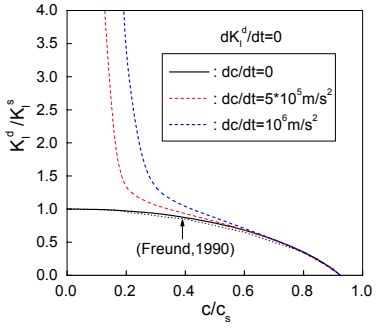

(a) Variation of acceleration

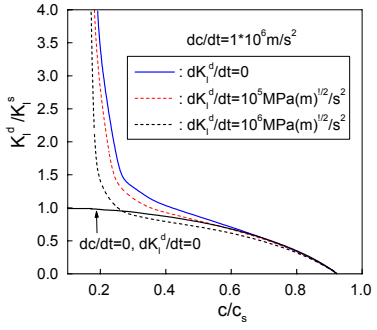

(b) Variation of time rate of change of DSIF

Fig. 6. The ratio of dynamic to static stress intensity factor versus normalized crack speed when a crack is propagating at a constant velocity or accelerating in an infinite plate under plane stress conditions and under the assumption that the crack propagates with a constant y-displacement at a point on the crack surface away from the crack tip.

stress intensity factor $\dot{K}_I^d$ when the crack propagates with acceleration. Unlike $\dot{K}_I^d = 0$, the normalized stress intensity factors can be determined, provided that a critical displacement v value to propagate crack is known. It is assumed that the critical displacement $v(\theta = \pi, r = 0.01 \text{ m})$ is 0.03 mm. The dynamic stress intensity factors change slightly when the displace-ment changes. As shown in Fig. 6 (b), the dynamic stress intensity factors decrease with increasing rate of change of stress intensity factor at a crack speed.

Figure 7 (a) shows the ratio of dynamic to static stress intensity factor versus normalized crack speed when a crack is propagating with deceleration under the Rayleigh wave speed in an infinite plate subjected to normal displacements. The stress intensity factors are not almost affected by acceleration at high crack speed $(c/c_s > 0.65)$. However, the stress intensity factors decrease rapidly when the crack propagates at low speed with high deceleration. Even if the crack

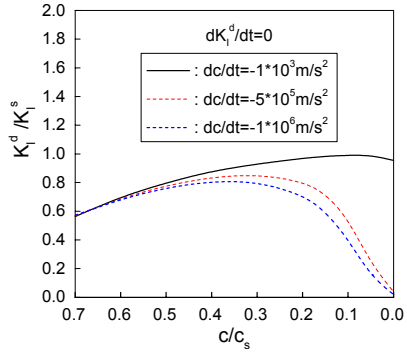

(a) Variation of deceleration

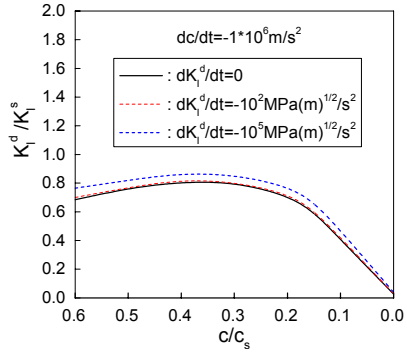

(b) Variation of time rate of change of DSIF

Fig. 7. The ratio of dynamic to static stress intensity factor versus normalized crack speed when a crack is propagating at a constant velocity or decelerating in an infinite plate under plane stress conditions and under the assumption that the crack propagates with a constant y-displacement at a point on the crack surface away from the crack tip.

propagates at low speed, when the crack deceleration is low, the dynamic stress intensity factors approach the static state.

Figure 7 (b) shows the influence of stress intensity factor on the rate of change of mode I stress intensity factor $\dot{K}_I^d$ when the crack propagates with deceleration. In an experiment using a single edge cracked tensile plate reported by Arakawa et al.(2000), $\dot{K}_I^d$ has a negative value when a crack propagates with deceleration. Thus, a negative $\dot{K}_I^d$ is applied during the crack deceleration. As shown in Fig. 7 (b), the dynamic stress intensity factors decrease with increasing the rate of change of stress intensity factor when a crack propagates with deceleration.

4. Conclusion

In this study, the stress and displacement fields for

an unsteadily propagating crack are developed through an analytic method. Specially, the partial differential equations for the higher order terms of two wave potentials Φ and Ψ in the dynamic equilibrium can be transformed into the Laplace's equations whose solutions have harmonic functions. The method of this transform is first shown in this paper.

The structure of the stress and displacement fields obtained in this study is general and universal. The higher order terms in the fields are not directly affected by the stress intensity factors and are not separated into two terms of stress intensity factors and non-stress intensity factors. Generally, experimental methods used in fracture investigations employ such descriptions of stress field to extract the stress intensity factor from full-filed experimental data sampled from a region between the near and far fields. In this intermediate region, a singular term and one or two higher order terms are sufficient to accurately describe a stress field. However, the analysis presented here indicates that at least three terms must be considered in the case of a transient crack in order to explicitly account for the transient effects. Using the transient stress fields developed in this study, the characteristics of the transient effects are shown. The results indicate that the isochromatic fringes of mode I tilt backward around the crack tip with increasing crack tip acceleration $\dot{c}$ and tilt forward around the crack tip with increasing the rate of change of the dynamic mode I stress intensity factor $\dot{K}_I^d$. When a crack propagates with a constant y-displacement at a point on the crack surface away from the crack tip, the stress intensity factors for a propagating crack in an infinite plate decrease as a crack speed increases, and become zero when a crack velocity approaches Rayleigh wave speed. Specially, when the crack propagates with suddenly high acceleration or deceleration at low velocity, the stress intensity factors increase infinitely or approach zero. However, the stress intensity factors are not almost affected by acceleration or deceleration at high crack speed $(c/c_s > 0.65)$. The dynamic stress intensity factors decrease with increasing the rate of change of stress intensity factor at a crack speed and increase with decreasing the rate of change.

Reference

Arakawa, K., Mada, T., Takahashi K., 2000, "Correlations among Dynamic Stress Intensity Factor, Crack Velocity and Acceleration in Brittle Fracture," *Int. J. of Fract,*. Vol. 105, pp. 311~320.

Chen, E. P., 1978, "Sudden Appearance of a Crack in a Stretched Finite Strip," *J. of Appl. Mech.,* Vol. 45, pp. 277~280.

Craggs, J. W., 1960, "On the Propagation of a Crack in a Elastic Brittle Materials," *J. Mech. Phys. Solids,* Vol. 8, pp. 66~75.

Freund, L. B., 1990, Dynamic Fracture Mechanics, Cambridge Univerisity Press, Cambrage.

Itou, S., 1980, "Transient Response of a Finite Crack in a Half Plane under Impact Load," *J. of Appl. Mech.*, Vol. 48, pp. 534~538.

Lee, K. H., Hawong, J. S., Choi, S. H., 1996, "Dynamic Stress Intensity Factors K_1, K_{11} and Crack Propagation Characteristics of Orthotropic Materials," *Engng. Fract. Mech.*, Vol. 53, No. 1, pp. 119~140.

Nisioka, T., Atluri, S. N., 1983, "Path-Independent Integrals, Energy Release rate and General Solutions of Near Tip Fields in Mixed-Mode Dynamic Fracture Mechanics," *Engng. Fract. Mech.*, Vol. 18, pp. 1~22.

Ravi-Chandar. K., 1993, "Experimental Measurement of dynamic Crack-Tip Stress-Field Parameters under Transient Loading," *Optics and Lasers in Engineering* , Vol. 19, pp. 141~159.

Rosakis, A. J., Liu, C., Freund, L. B, 1991, "A note on the Asymptotic Stress Field of a Non-Uniformly Propagating Dynamic Crack," *Int. J. of Fract*., Vol. 50, pp. R39~R45.

Sih, G. C., Embley, G. T., 1972, "Impact Response of a Finite Crack in a Plane Extension," *Int. J. of Solids Structures*, Vol. 8, pp. 977~993.

Thau, S. A., Lu, T. H., 1971, "Transient Stress Intensity Factors for a Finite Crack in an Elastic Solid Caused by a Dilatational Wave," *Int., J. Solids Structures,* Vol. 7, pp. 731~750.